Designing Arm for Placement of an Impact Hammer in Sewers

Beck Wittenstrom

Thursday 6th June, 2019

Contents

Summary

Underground sewer pipelines need maintenance from sources of damage, such as unstable ground support. To mitigate this the TISCALI project (Technology Innovation for Sewer Condition Assessment using Long-distance Information-systems) is creating an impactor sensor to look for early warning signs of collapse. We designed a 4 joint arm to place the impactor at a specific position and orientation in relation to the sewer wall. Then, we developed a control system for the arm to place the impactor while avoiding collision with the sewer wall. Finally, different systems were explored to mitigate recoil from the impactor, and we chose a non-backdrivable gear system. The arm can place the impactor in various pipe sizes and avoid collision with the sewer wall by using a path generation algorithm. Finally, recoil is limited to 0.2mm via the non-backdrivable gear system.

Preface

I would like to thank Hengameh Noshahri for supervising me during this project and Stefan Groothuis for volunteering his time to help me.

Beck Wittenstrom

1 Introduction

1.1 Problem Context

The Nethlands has more than 90,000 kilometers of sewer lines (The Ministry of Infrastructure and Water Management,2019). These lines need maintenance and repair. This is because aging infrastructure is leading to increased risk of sewer failure(Davies et al., 2001). Preventing sewer failure is much better than repairing broken sewers. This is because damage in a sewer pipe collapse usually starts with a small defect, which if not repaired can cause the pipe to collapse. So, there are many opportunities to prevent complete collapses. Meanwhile if the pipe is repaired after the collapse these failures can stay buried for years before they are uncovered and fixed. Finally, the repair process is expensive and time-consuming. This is because to identify where the collapse is and repair it, large sections of pipe must be dug up (Ana and Bauwens, 2007). To avoid expensive repairs small defects can be identified and collapse prevented. To implement defect detection in-pipe robots have been created to move through sewer pipes carrying sensors and tools to find and fix defects.
The TISCALI project(Technology Innovation for Sewer Condition Assessment using Long-distance Information-systems) is creating a sensor that uses the impact echo-method to detect defects. The impact-echo method uses a hammer to create a to generate stress waves in the sewer wall, while a transducer records the surface displacement due to reflected and direct stress waves. The reflected waves give information about the integrity of the element, such as flaw detection. The sensor, called the impactor, will look for early warning signs of sewer decay.

1.2 Problem Statement

In order for the impactor to find defects, it must apply a specific amount of energy to the sewer wall. This is important because the impact energy must be high enough to create stress waves with sufficient amplitude and frequency content. In order to consistently apply the same energy, it must be placed and kept normal to and at a specific distance from the sewer wall. A consistent distance and orientation will allow the impact energy to be calibrated.
The aim of this assignment is to design an autonomous arm that can be attached to an in-pipe robot. The arm must be able to place the impactor accurately and keep it in that position to allow the impactor to apply consistent impact energy. To place the end effector the workspace must be equal to or larger than the sewer with a diameter of 375mm. This is to allow the impactor to be placed striking distance of the wall in any pipe. The in-pipe robot will roll along cylindrical sewer pipe with a diameter from 150 to 375mm. This means that the base of the arms base is not always in the center of the sewer. Finally, to keep the impactor in place even as it fires, the arm should minimize the movement caused by impulse applied to the arm by the impactor. This is hereafter known as recoil. The whole arm will be made of a chain of joints and links exemplified in Figure 1.1. The arm can be modeled abstractly by Figure 1.2 where the arm's dynamic model is represented by the Plant, The Control system is represented by the controller and the recoil mitigation system is represented by the feedforward controller.

1.3 Organization of the report

In section 2 the arm designs are presented. The second section investigates different joint configurations for the arm. Then, the best arm for the application is chosen and a dynamic model is built. Finally, that model is tested for accuracy. In section 3 the utility of different control systems are analyzed. Then a system is chosen, implemented and tested. Finally, in section 4 a recoil mitigation system is chosen for the arm.

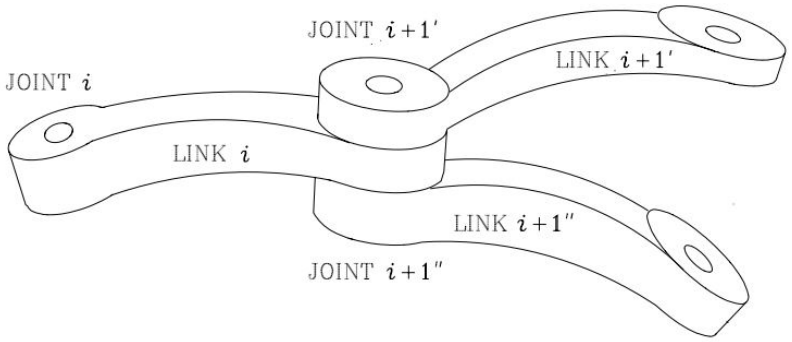

Figure 1.1: Joint link representation and naming convention.(Siciliano et al., 2010)

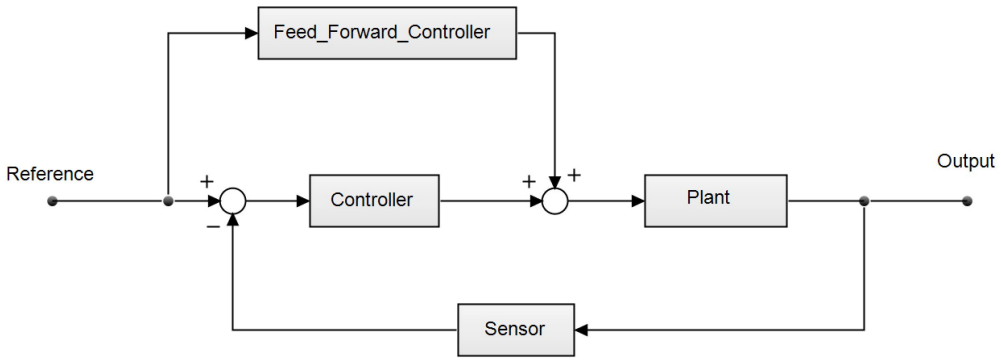

Figure 1.2: FeedForward Feedback Control Model: The plant is the dynamic model of the arm, Sensor represents the behavior of the sensors to the output variables they measure, the Controller and Feedforward Controller represent the system that decides on inputs to the plant to match the output to the reference

2 Arm Design

2.1 Analysis

2.1.1 Kinematic Chains

An arm can be looked abstractly as a kinematic chain of rigid bodies(links) connected by joints. The position and orientation of the joints can be described by a frame of reference pertaining to that joint. The relation between these joints are described by transformation matrices that relate each of the frames of reference. For example, the pose of joint 1 is represented by Ψ_1 and the pose joint 2 by Ψ_2. Then the relation between these two joints is represented by $\Psi_1 = H_2^1 \Psi_2$. Finally, Ψ_e represents the frame of reference of the end effector; this is the frame that must be positioned and orientated as it represents the impactor. Finally, x_e of Ψ_e is the direction of the impactor stroke.

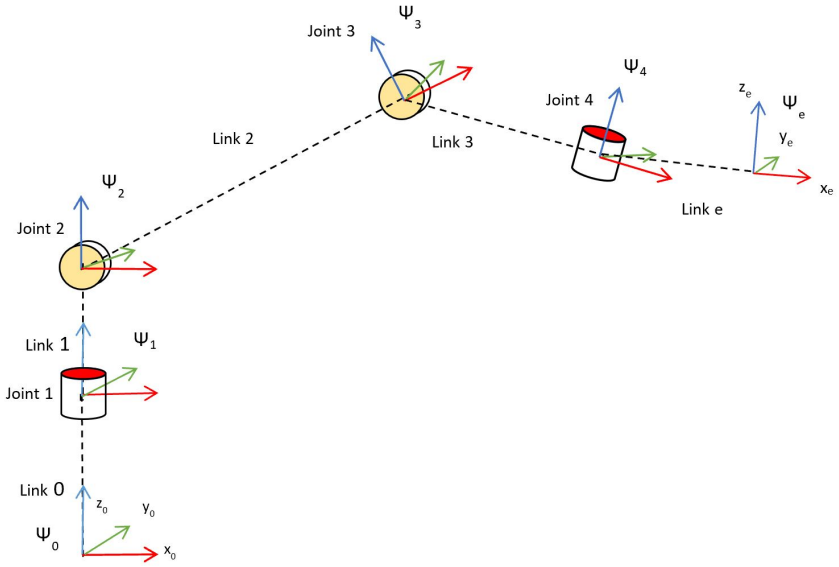

Figure 2.1: 4-DOF kinematic structure with Ψ_0 the base frame

2.1.2 Joint Configuration

To achieve complete freedom of orientation and position of the end effector a robot arm needs six degrees of freedom(DOF) (Siciliano et al., 2010). This is because it needs one DOF for each axis of movement and rotation. However, in this application, the robot arm does not need all 6 DOF. This is because the impactor only needs the direction of the impactor stroke, x_e, to be normal to the sewer wall. So, the orientation of z_e and y_e do not need to be independent from the position of the end effector. Also, the in-pipe robot, which acts as the base of the arm or ψ_0, can move parallel to the pipe giving the arm a DOF. So, the arm needs 4 DOF as one DOF is not needed and one DOF is provided by a moving base. To give the arm 4 DOF it needs a minimum of 4 joints(Siciliano et al., 2010). The arm should only have the minimum number of joints, as it does not need extra degrees of freedom to avoid obstacles. There are 4 types of joints including, roll, yaw, and pitch revolute joints, as well as translational joints. Since, the arm needs 4 joints and there are 4 choices for every joint there are 256 possible designs. The number of choices can be narrowed down through four design heuristics. The first heuristic is

that yaw and pitch joints are not optimal as the first joint in a chain because their movement is constrained by collision with the base. This means that the first joint should be a roll joint as seen in Fig 2.2. Second, Two roll joints in a row add no degree of freedom to the robot. So, Joint 2 could be either pitch or yaw joint. The third rule is that after a roll joint, pitch and yaw joints are effectively the same (Huttenhuis, 2015). So, all the arms with pitch or yaw joints as the second joint can be considered the same arm. Fourth, the last joint cannot be a roll joint as it would waste a degree of freedom. This is because the impactor does not need rotation about the X-axis of the end effector frame, as shown in Figure 2.1. If the last joint were a roll joint this would cause a loss in useful degrees of freedom. Any arm design with a prismatic joint that is parallel to the sewer pipe is redundant because of the arms base already moves in that DOF. This leaves prismatic joints that are perpendicular to the pipe. These joints are not preferred for this application as they offer no advantage in terms of recoil mitigation. They also have problems meeting workspace requirements, as typical prismatic joints can only extend to double there size by moving a slider along a shaft. It is possible for the workspace to be extended using more complicated telescoping joints. However, these make the system contain more moving parts which lead to a lack of reliability (Siciliano et al., 2010). Since there is no advantage to prismatic joints and there is are downsides to meeting workspace requirements or adding to mechanical complexity by using telescoping methods such as in Figure A.1 it is preferable to choose between arms with only revolute joints. By removing designs using prismatic joints and violating the arm design heuristics this leaves two joint configurations shown in Fig 2.3. Using the 4 design heuristics and removing prismatic joints the design choices are reduced down to arm type 1 and 2 seen in Figure 2.3.

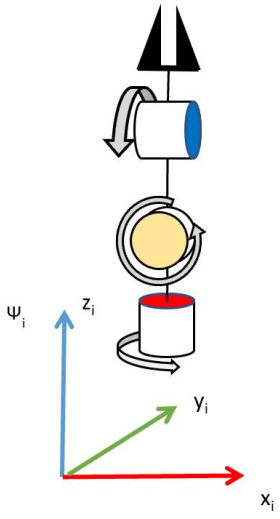

Figure 2.2: Roll- Yaw- and Pitch- joints with there positive direction of rotation(Huttenhuis, 2015)

2.1.3 Link Size

The choice of arm design depends on the choice of link lengths. The link lengths should allow the arm to place the end effector normal to the wall and within 30mm from it as this is the maximum stroke length of the impactor. The maximum distance that the arm will need to place the impactor from the center of 150mm sewer to the top of the sewer or 300mm. So, the total length of all links should be 300mm in order to be able to reach there. Meanwhile, the combination of link 3 and the end effector must be smaller than 100mm in order to fit in the

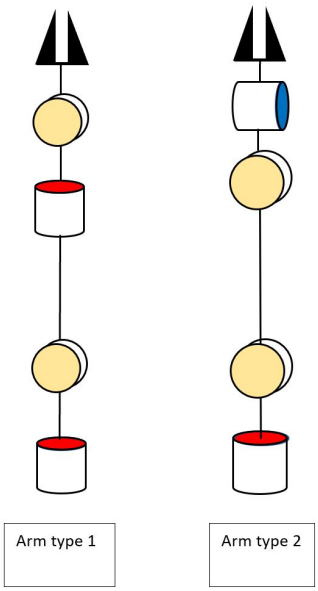

Figure 2.3: 2 different arm designs made from Roll, Pitch, and Yaw joints

smallest sewer of 150 mm and place the end effector 30 mm away from the wall, and have a 20mm safety zone in order to not bump into the sewer wall. Then this means that link 1 is 300mm-100mm so should be 200mm long. In order to choose link 3 and 4 an arm type must be chosen. This is because arm type 1 must have link 4 cover the complete 100 mm as any length to link 3 will just be an extension of link 2. Meanwhile arm type 2 can have link 3 be 70mm and the end effector length be its minimum of 30mm. This improves the accuracy of placement as the angular inaccuracy of the joint 4 has a reduced effect on the positional inaccuracy of the end effector, because it is closer to the end effector. The advantage of Arm type 1 is that it has improved reach. This is because in order to take a specific orientation joint 4 in arm type 2 must bend reducing the total distance between the end effector and joint 3. However, this extra reach does not matter as the workspace of both arms are much larger than the size of the sewer. This is because to reach the top of the sewer the arm must be able to reach from the top of the in-pipe robot to the top of the sewer or a distance of 300mm, which gives a circular workspace with a diameter of 600mm. So, arm type 2 is a better choice for this system, as it has an equivalent useful reach and improved accuracy compared to arm type 1. Arm type two should also be implemented with link lengths 0, 200, 70 and 30 mm respectively. This combination of joints and links attached to the in-pipe robot creates a workspace of 600mm cylinder which completely envelopes the maximum needed workspace of 375mm diameter cylinder. The fourth joint will always be able to position the end effector normal to the wall because the reduced reach caused by the fourth joint turning is rendered moot by the extra workspace.

2.2 Design

There are various options in order to model the dynamic behavior of an arm. These include Lagrangian, and Newton-Euler formulation as well as bond graphs. All of these methods create equivalent models however some are more computationally efficient than others(Siciliano et al., 2010). Bond Graphs will be used to model the arm since computational efficiency is not a concern and the author is more familiar with bond graph modeling. Bond Graphs are a method of dynamic modeling based on energy and energy transfer, which allows domain independent modeling. For, example capacitors and springs both store potential energy, meanwhile, induct-

ors and masses both store kinetic energy.
The model of the arm 2 consists of four rigid bodies connected with ideal joints. The rigid bodies were all assumed to have the shape of a rectangular prism with homogenous density and a base of 20x20mm and a length pertaining to the link that the rigid body represents. The mass of link 2 and 3 were calculated using a density of 1.05 grams per centimeter cubed as this is about the density of 3d printed plastic which is expected to be used in a fast prototype. However, material choices and link shape design are beyond the scope of this project. The end effector or link 4 has a mass and shape that are determined by the solenoid used by the Tiscali project a, Red Magnets ITS-LS 5852 linear solenoid.
The rigid bodies were then represented in 20sim by the twist of the bodies center of mass in the body-fixed frame connected to its inertia matrix. The bodies have 3 forces applied to them, gravity, the fictitious forces from the bodies moving frame of reference and the normal forces from the joints. Gravity is modeled as a source of effort directed in the negative Y-axis of the global frame as shown in Figure 2.1. The MGY in Figure 2.4 calculates the fictitious forces caused by the movement of the bodies frame of reference. The normal forces of the joints were modeled by constraining the bodies motion relative to each other using Springs and resistances with values of 10^9 in all degrees of freedom besides the joints DOF. These large values were chosen to mimic rigid joints the displacement of these springs will very small and can be considered zero Folkertsma (2018). Two joints of the complete model can be seen in Figure 2.4 in the Joints Models section.

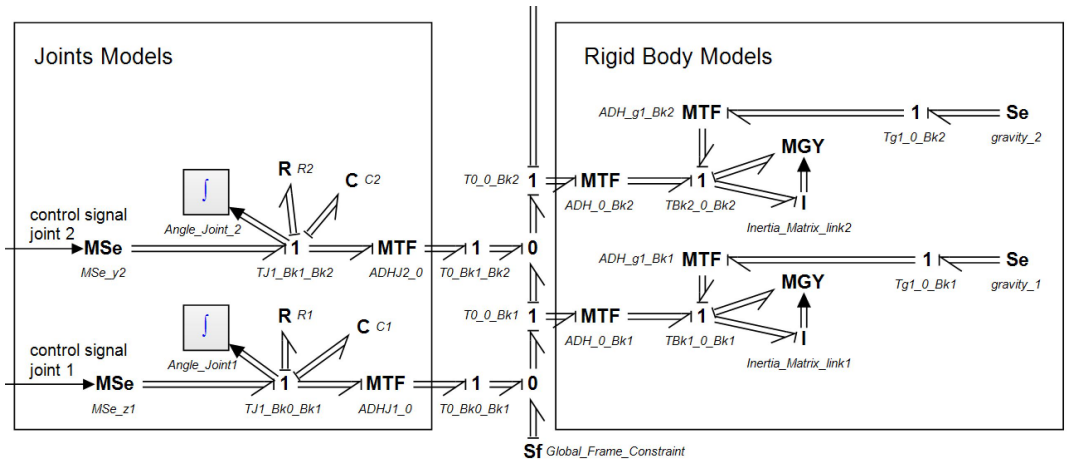

Figure 2.4: TA B C is the twist of B w.r.t C in the frame of A. The MTF components represent the twists and wrenches being transformed to a different frame of reference for example (ADHJ1 0) from J1 to the global frame 0

2.3 Results

In order to verify the model two tests were made. One to verify the validity of the joint model, and the other to verify the validity of the gravitational forces, and fictional forces. In the first test the arm was given a simple integral controller to hold the arm perpendicular to gravity. The results of this test show that joint one bears a load of 4.3599N and joint 4 bears a load of 0.1612764N seen in Figure 2.5. These are exactly equal to the expected forces when the static loads are calculated for these two points.

The second test verifies the force of gravity in the body and the fictitious forces. In the test, all joints are locked in position along the global x-axis except for the fourth joint. The fourth joint is spun at a constant rate of πrad every 10 seconds around the global z-axis. The expected result is a cosine and sine function for the body-fixed frame forces. Meanwhile, the fictitious forces are expected to have a constant positive force in the x-axis of the body-fixed frame. These

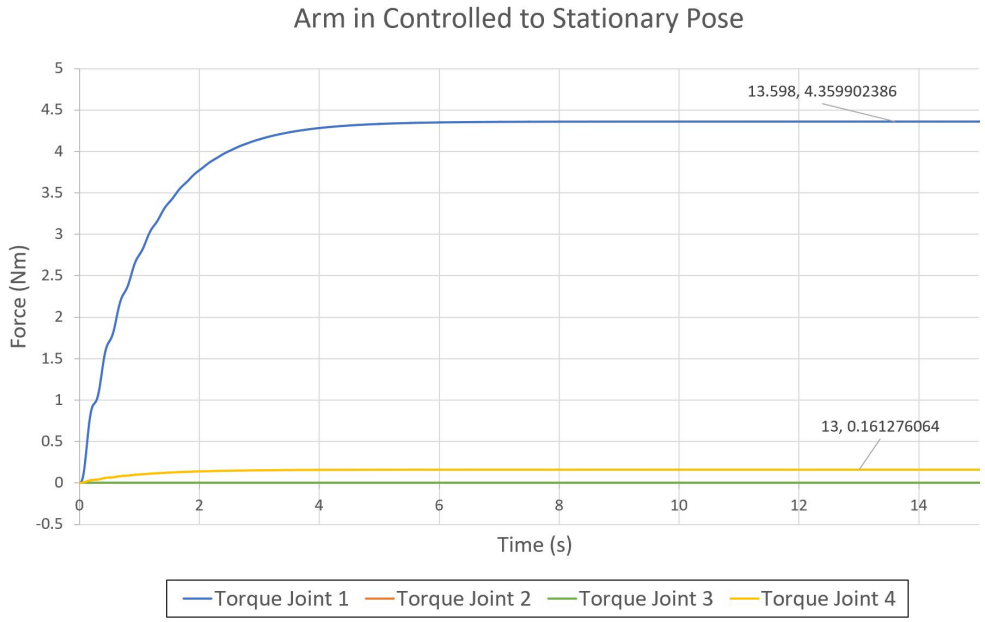

Figure 2.5: The torque applied to each joint to keep the arm in stationary pose with all links parallel to the global x axis and perpendicular to the force of gravity.

results are confirmed in Figure 2.6 and Figure 2.7. Thus, the models accuracy can be confirmed

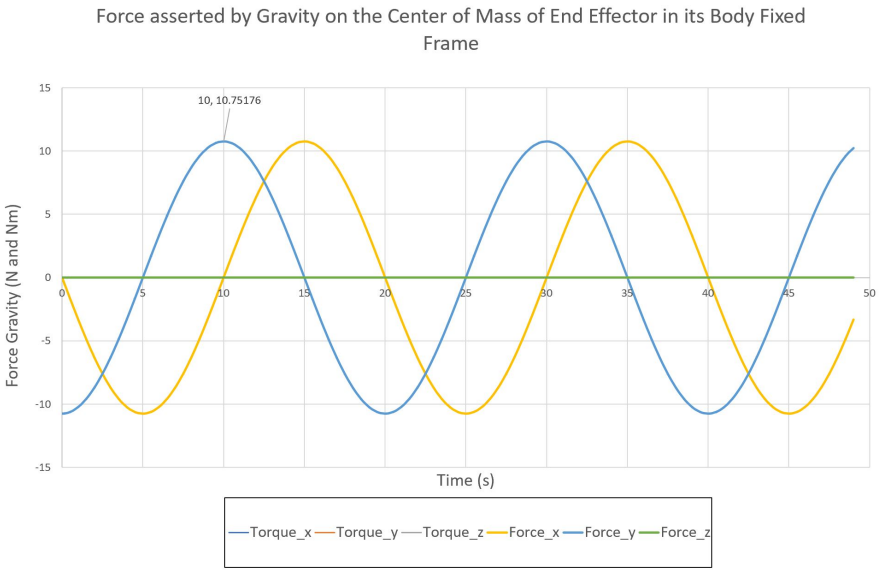

Figure 2.6: The force of gravity on the center of mass of the end effector as it rotates at one tenth pi radians per second

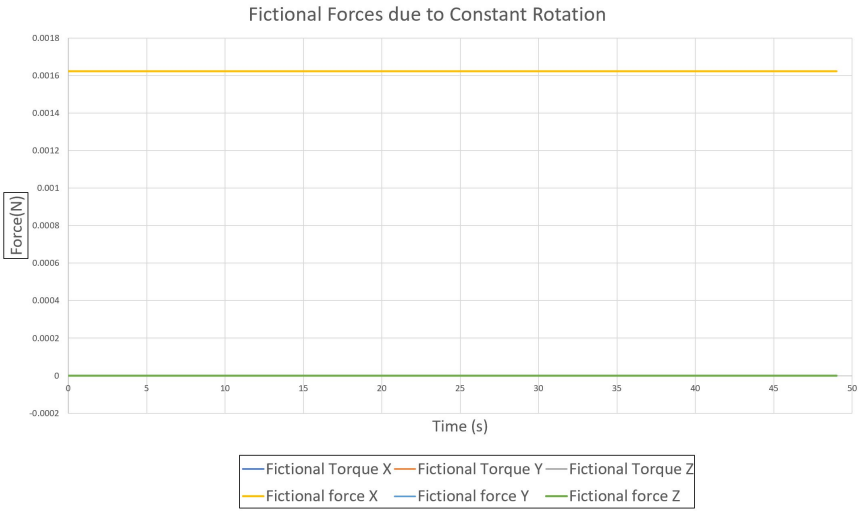

Figure 2.7: Ficticious forces on the end effectors center of mass in the body fixed frame

3 Control System Design

3.1 Analysis

The requirements for the control system are that it needs to achieve high accuracy, fast settling time, and must never allow the arm to collide with the sewer walls. The options for control systems include Centralized control, virtual springs, and independent inverse Kinematic Control. Centralized control methods include dynamic effects into the control system rather than treating them as disturbances. They are necessary for high-velocity applications which this arm does not need to achieve (Siciliano et al., 2010). So, option one is a virtual spring controller. It moves the end effector to the reference by requesting a wrench on the end effector that is proportional to the difference between the reference pose and pose of the arm. This Wrench then is converted to torques on the actuators through the transpose of the Jacobian matrix of the arm(A.0.2). This method has the advantage that it pushes the end effector directly to the reference location. However this method does have issues around singularities as the rank of the Jacobian is reduced, thus reducing mobility. There are two types of singularities: boundary singularities and internal singularities (Siciliano et al., 2010). Boundary singularities are caused by the arm reaching full extension, meanwhile, internal singularities appear when different joints along the arm align. While boundary singularities are usually not an issue as the arm's length can be increased or the boundaries can be avoided(Siciliano et al., 2010). In this situation though, the increase in the length of the arm will increase the arms susceptibility to recoil from the impactor, as the increased length of the arm will increase the torque on the joints created by the impactors impulse.
The second choice for the control system is independent inverse kinematic control. This system first calculates the position of each joint necessary to achieve the desired end effector pose. Then, it applies a torque proportional to the difference between the desired joint position and the current joint position. The disadvantage of inverse kinematics equations is that they may have many solutions or infinite solution. They also may have no solutions as they are generally non-linear (Siciliano et al., 2010). Due to the existence of singularities, and the relative ease at which inverse kinematic equations can be solved with only 4 joints, the inverse kinematic method was chosen as the way to control the arm.

3.2 Design

To implement this control system a reference signal determined the desired position of the end effector in the x and y of the global frame as well as the rotation around Z and Y in the global frame. This created a system of equations seen in A.0.2 that could be solved resulting in four solutions. However, three of these solutions would result in a collision with the base. So, one solution was chosen using the constraints that the end effector should not point back toward the base, and that joint 2 will collide with the base if it rotates below the x y plane. Another problem was that independently moving joints caused the end effector to not always follow a path that would avoid collision with the wall of the sewer. To avoid this, a simple path generation algorithm was implemented, that moves the reference from the initial pose to the desired pose in discrete steps. Each of the 4 reference signals, the x, and y position as well as Y and Z rotation are moved using the equation below. Ref_i is the initial reference or current pose, Ref_e is the desired pose and Ptime is the time to complete the path. Finally, T is the simulation time, which is limited to $0 < T < Ptime$.

$$ref = \frac{(Ref_e - Ref_i)T}{Ptime} + Ref_i$$

So when T is 0 the $ref = Ref_i$, but when $T = Ptime$ then $ref = Ref_e$. After the reference signal for the end effector is generated it is converted to a joint angle for each joint. Then,

a proportional control was applied to each joint. This led to inaccurate steady state values. Thus an integral control was added. Another issue was that when path passed over the origin joint one would need to turn 180deg instantly. This would cause the arm to turn quick and the end effector woruld swing out due to centrifugal force. To reduce this a resistance control was added. The values were then tuned manually with the proportional coefficient being 100 and the derivative coefficient being 10 for each joint. Finally, there was a problem with integral windup as the arm moved to the desired pose reference. To fix this the integral control is only applied once the final reference is applied. So, the controller is a PD controller as the end effector follows the path to the final reference. Then, when $T = Ptime$ the end effector needs to be moved accurately into the final position the integral controller is applied. This removed integral windup and thus reduced overshoot.

3.3 Results

To test the controller, I created an example path that moves the end effector's position from (0.2,0.2) to (0.2,-0.2) and changes its rotation around the Z-axis from 90deg to 0 deg.Fig 3.1 shows the path of the end effector's position in 3 dimensions as it followed the reference. Meanwhile, Fig 3.2 shows the simulated positional error of the end effector in the X_0 and Y_0 axis over time. The reason why the line is thick from 0.3 seconds to 10 seconds as the reference is jumping every 0.01 seconds causing the error to oscillate quickly. The settling time is 15 seconds then the error dips below a thousandth of a millimeter. The maximum error is under 4 millimeters which ensure that the end effector will not contact the wall as the impactor is currently being calibrated to fire 14 mm from the wall. If the impactor needs to be positioned closer to the wall than 4 millimeters, the controller will need to be adjusted. The new controller will need to follow the path more precisely.

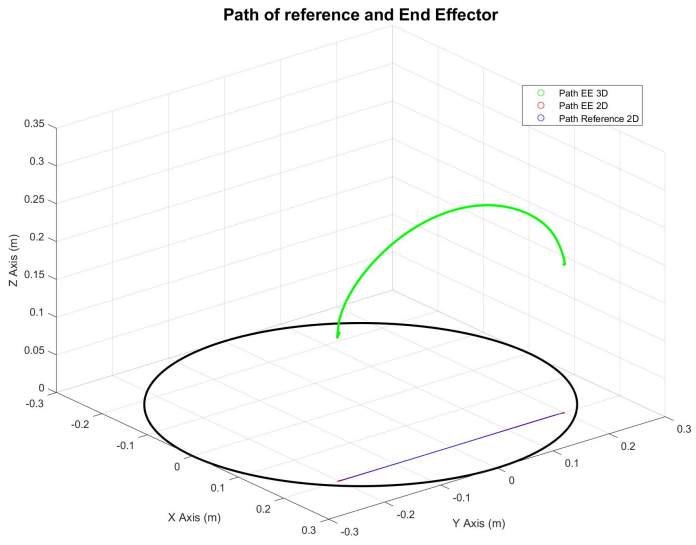

Figure 3.1: The path of the end effector, while following a path from from (0.2,0.2) to (0.2,-0.2) with end effector angle changing from 90deg to 0 deg rotated around the Z axis

Figure 3.2: End effector position error in the X and Y axis, while following a path from from (0.2,0.2) to (0.2,-0.2) with end effector angle changing from 90deg to 0 deg rotated around the Z axis

4 Recoil Mitigation System Design

4.1 Analysis

To test the effect of recoil on displacement we added a linear actuator to the end of the end effector. The End Effector link was split into two masses of 0.616kg for the casing and 0.480 for the hammer. The mass of the hammer was estimated by calculating the mass of a steel cylinder with dimensions from the ITS-LS 5852 data sheet. Then the mass of the casing was calculated via the difference of the hammer and total mass of the linear solenoid. The actuator was then given a pulse source of effort that applies a maximum force of 85 newtons. The force of the actuator reduces linearly to 35 newtons at the actuators max stroke length of 30mm, just like the ITS-LS 5852. When the actuator fires it applies the force to the hammer, and a reactive force to the arm. The reactive force moves the arm taking energy from the eventual impact. This is recoil. The recoil test placed the end effector so that the reactive force would be tangential to joint 2 creating the most torque and thus the most movement.
In order to reduce the effect of recoil, the end effector must be able to stay in the same position

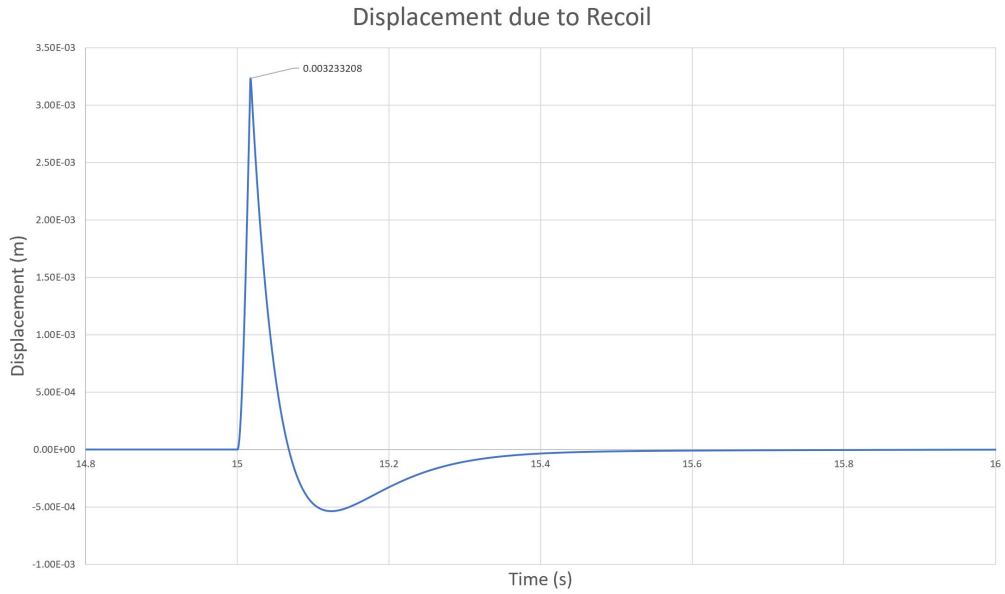

Figure 4.1: Effect of recoil on end effector displacement along the X axis of the body fixed frame of the end effector

despite an external impulse from the impactor. The impactor firing will create torques on joint 1 and 2. This is because joint 3 and 4 will always be normal to the direction of recoil, so recoil will cause no tangential force on the revolute joints to create torque. The torques experienced by joints 1 and 2 can be negated by either a feedforward controller applying counter force or a brake to apply a normal force. The effectiveness of a feedforward controller depends on the accuracy of the model. Meanwhile, a brake provides a normal force and will cancel any disturbance as long as the disturbance is smaller than the locking force. Since brakes will achieve the same result as a feed-forward control, but without the need for precise models, a brake is a better option for recoil mitigation. There are many types of brakes. They can generally be grouped into mechanical, friction, or singularity locks (Plooij et al., 2015). These categories can be split into passive or active systems this can be seen in Fig. 4.2. The lock for this arm must be able to lock in any position, as the impactor must be able to locked into any position in the workspace. The lock also must be smaller to be than a 150mm circle, in order to fit inside the

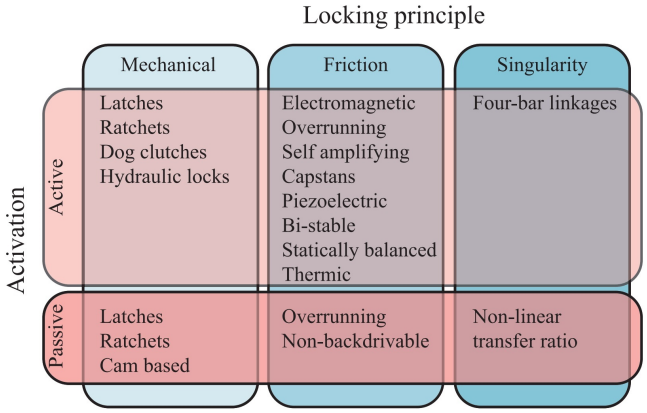

Figure 4.2: Classification of locking devices into three categories. All three can be divided into actuated and non actuated devices(Plooij et al., 2015)

sewer tunnels. Finally, the lock must be able to stop a torque of 26.57Nm from the recoil in addition to the force of gravity on the joints. Given the requirements for torque and infinite lock positions, the best choices are self-amplifying brakes or non-backdrivable gears.
Non-backdrivable gears are closer to an ideal brake in terms of size than self-amplifying brakes(Plooij et al., 2015). They also have the advantage of being a passive system. This means that it does not need energy to lock so the arm can be locked in a position indefinitely while the in-pipe robot moves through the sewers. One problem with non-backdrivable gears is that they are susceptible to backlash. Based on backlash values that have been found in catalogs of precision gears, a radial backlash value of 0.00087radians is a reasonable value for a worm gear (ConeDrive, 2019). If the pose is in the same worst-case scenario where link 2 is parallel to the sewer/ the global z-axis, the maximum movement would be 0.2mm normally away from the sewer wall. A simulation would not be a good test for this system as it depends heavily on real-world constraints such as manufacturing precision and wear of the gear. So, This topic should be explored further by another project.

5 Conclusion

5.1 Context

The presented arm is a 4 joint serial chain with 4 revolute joints, and 4 links of lengths 0m, 0.275m, 0.70m, and 0.03m. In a 20sim simulation the control system uses inverse kinematics and path generation to position the end effector while following a path with 7mm of error . Finally, two non-backdrivable gears attached to joint one and two limit recoil at an estimated 0.2mm. The arms configuration fulfills the requirements to be able to place the impactor normal to any part of the sewer wall. The control system places the end effector without collision, and the non-backdrivable gears reduce recoil to allow for precise impacts. While the arm fulfills the requirements of this project it is not ready for implementation.
The non-backdrivable gears are a good theoretical solution, but futher investigation is required. The non-backdrivable gears should be implemented to test their practical feasibility in terms of precision, maintenance, and cost. Also, because the arm cannot sense the size of the sewer, it cannot position itself relative to it. Thus, a system must be developed to discern the size and layout of the sewer. This could be done by having the arm find the distance to the wall through contact or by using a range finding sensors such as lidar, or sonar.

A Appendix 1

A.0.1 Arm design

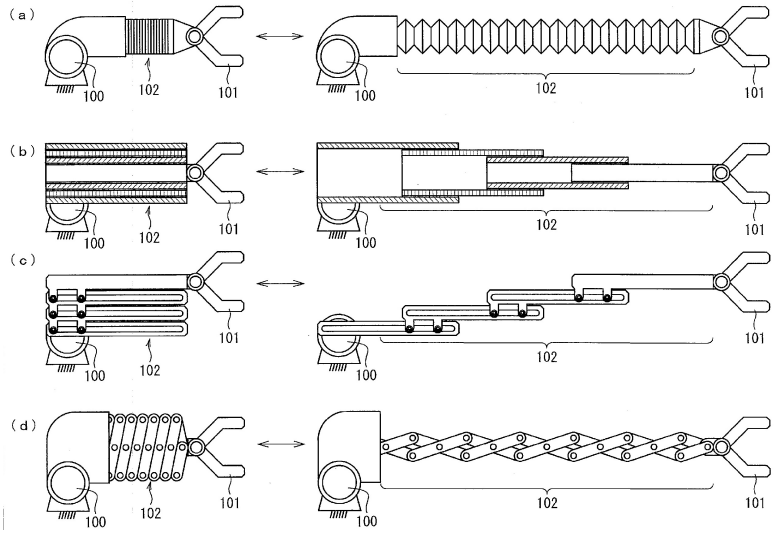

Figure A.1: Various types of telescoping joints to improve the size to stroke length ratio(Ichiro et al., 2010)

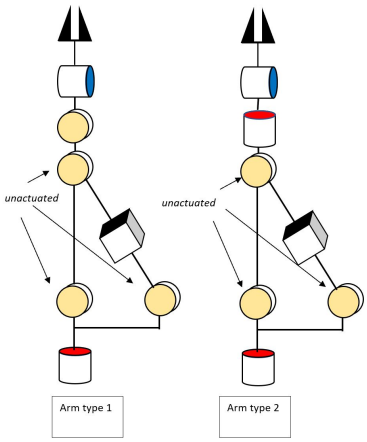

Figure A.2: two arm designs using prismatic joint and 3 unactuated yaw joints

A.0.2 Control design

Inverse Kinematic system of equations $x^0_{u_e}$ is the x unitvector of the end effector frame in the global frame $y^0_{u_e}$ is the y unitvector of the end effector frame in the global frame x^0 is the x position of the end effector frame in the global frame y^0 is the y position of the end effector frame in the global frame

$$x^0_{u_e} = Cos[a]Cos[b+c]Cos[d] - Sin[a]Sin[d]$$

$$y^0_{u_e} = Cos[b]Cos[c]Cos[d]Sin[a] - Cos[d]Sin[a]Sin[b]Sin[c] + Cos[a]Sin[d]$$

$$x^0 = Cos[a](L2Cos[b] + L3Cos[b+c])$$

$$y^0 = (L2Cos[b] + L3Cos[b+c])Sin[a]$$

Transpose of the jacobian

-(L2 Cos[b] + L3 Cos[b + c]) Sin[a]	-(L2 Cos[b] + L3 Cos[b + c]) Sin[a]	-(L2 + L3 Cos[c]) Sin[a]	-L3 Sin[a]
Cos[a] (L2 Cos[b] + L3 Cos[b + c])	Cos[a] (L2 Cos[b] + L3 Cos[b + c])	Cos[a] (L2 + L3 Cos[c])	L3 Cos[a]
0	0	0	0
0	0	Cos[a] Sin[b]	Cos[a] Sin[b + c]
0	0	Sin[a] Sin[b]	Sin[a] Sin[b + c]
1	1	Cos[b]	Cos[b + c]

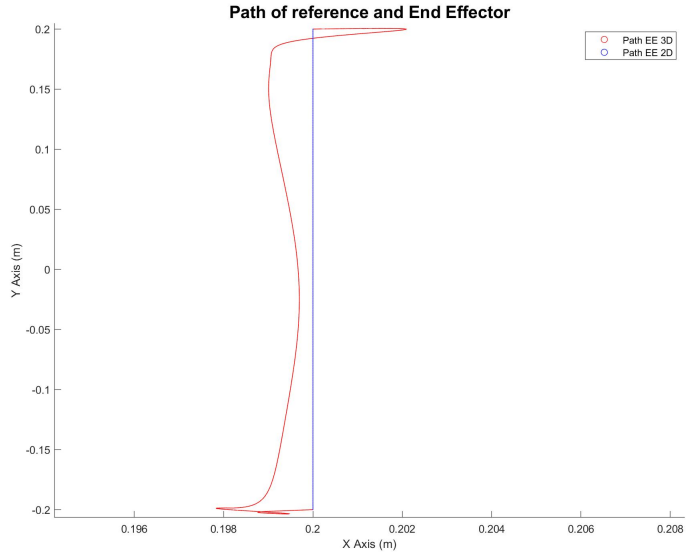

Figure A.3: The Path of the end effector, while following a path from from (0.2,0.2) to (0.2,-0.2) with end effector angle changing from 90deg to 0 deg rotated around the Z axis

Bibliography

Ana, E. and W. Bauwens (2007), Sewer network asset management decision-support tools: a review, in *International Symposium on New Directions in Urban Water Management*, pp. 1–8.

ConeDrive (2019), Product Range.
http://conedrive.com/wp-content/uploads/2019/01/Product-Range.pdf

Davies, J., B. Clarke, J. Whiter and R. Cunningham (2001), Factors influencing the structural deterioration and collapse of rigid sewer pipes, **vol. 3**, no.1, pp. 73 – 89, ISSN 1462-0758, doi:https://doi.org/10.1016/S1462-0758(01)00017-6.
http://www.sciencedirect.com/science/article/pii/S1462075801000176

Folkertsma, J. E. . G. (2018), Control for UAVs.

Huttenhuis, J. A. J. (2015), *Kinematic Design Method for a Rail Mounted Inspection Robot Arm*, Master's thesis, University of Twente, HORST BUILDING, NR. 20 POSTBUS 217 7500 AE ENSCHEDE THE NETHERLANDS.

Ichiro, K., Y. Woo-Keun and T. Kotoku (2010), Linearly Moving Extendable Mechanism and Robot Arm Equipped With Linearly Moving Extendable Mechanism.
https://patentscope.wipo.int/search/en/detail.jsf?docId=WO2010070915

Plooij, M., G. Mathijssen, P. Cherelle, D. Lefeber and B. Vanderborght (2015), Lock Your Robot: A Review of Locking Devices in Robotics, *Robotics Automation Magazine, IEEE*, **vol. 22**, pp. 106–117, doi:10.1109/MRA.2014.2381368.

Siciliano, B., L. Sciavicco, L. Villani and G. Oriolo (2010), *Robotics Modelling, Planning and Control*, Springer-Verlag London Limited, ISBN 0134456789.